



Fluorenylvinylenes bridged triphenylamine-based dyes with enhanced performance in dye-sensitized solar cells

Huipeng Zhou^a, Pengchong Xue^a, Yuan Zhang^b, Xin Zhao^a, Junhui Jia^a, Xiaofei Zhang^a, Xingliang Liu^a, Ran Lu^{a,*}

^aState Key Laboratory of Supramolecular Structure and Materials, College of Chemistry, Jilin University, Changchun 130012, PR China

^bCollege of Chemistry, Beijing Normal University, Beijing 100875, PR China

ARTICLE INFO

Article history:

Received 13 June 2011

Received in revised form 26 August 2011

Accepted 6 September 2011

Available online 8 September 2011

Keywords:

Dye-sensitized solar cells (DSSCs)

Triphenylamine

Fluorenylvinylene

ABSTRACT

We have synthesized a series of new dipolar organic dyes **Bn** ($n=0, 1, 2$) employing triarylamine as the electron-donor, 2-cyanoacrylic acid as the electron-acceptor, and fluorenylvinylene as the conjugated bridge, which were used as sensitizers in dye-sensitized solar cells. It is found that the solar-energy-to-electricity conversion efficiencies of the prepared DSSCs are in the range of 2.79–5.56%, which reach 35–70% of a standard device based on **N719** fabricated and measured under the same conditions. The DSSC sensitized with **B1** with balanced length of conjugated bridge shows the highest photo-to-electrical energy conversion efficiency and the open-circuit photovoltage (V_{oc}) of 0.86 V.

© 2011 Elsevier Ltd. All rights reserved.

1. Introduction

In recent years, energy demands and global warming have aroused intense attention in clean renewable solar energy sources. In this context, dye-sensitized solar cells (DSSCs) have attracted considerable attention as they offer the possibility of low-cost conversion of photovoltaic energy.¹ Although the conventional ruthenium-based sensitizers (such as **N3/N719**)^{2,3} and the black dye⁴ hold the record of the solar-energy-to-electricity conversion efficiencies of 11% under AM 1.5 irradiation, they are expensive and hard to purify relative to metal-free organic sensitizers. Thus, organic sensitizers have emerged as competitive alternatives to the Ru-based counterparts because various organic chromophores with high molar extinction coefficients can be readily synthesized.⁵ Thus, considerable progress has been made on the design of organic dyes, which favor high performance in DSSCs.^{6,7} Recently, Wang and co-workers reported an impressive high conversion efficiency of 9.8% for a DSSC based on a D- π -A chromophore in which 3,4-ethylenedioxythiophene was used as a spacer linked to dihexyloxy-substituted triphenylamine electron-donor (D) and cyanoacrylic acid electron-acceptor (A).⁸ In addition, many reported DSSCs that utilize organic dyes, such as the derivatives of carbazole,⁹ phenothiazine,¹⁰ coumarin,¹¹ indoline,¹² cyanine,¹³

hemicyanine,¹⁴ merocyanine,¹⁵ perylene,¹⁶ thiophene,¹⁷ fluorene,¹⁸ and triarylamine,¹⁹ as the sensitizers have yielded good conversion efficiencies. It has been found that most of the efficient organic dyes employed in DSSCs generally contain donor and acceptor bridged by a π -conjugated linker (D- π -A), and tuning of the length and torsion angle of the conjugated linker is important in increasing the molar extinction coefficient and realizing panchromatic light-harvesting. For example, the linker of styrene,²⁰ furan,²¹ vinyl,²² thiophene²³ or thienothiophene²⁴ incorporated into the triarylamine-based organic framework could enhance the efficiency. As a well-known conjugated unit, fluorenylvinylene has been extensively studied in functional organic materials (including emitting, nonlinear optical and liquid crystal materials, etc.),²⁵ however, it has not been used as a spacer in triphenylamine-based dyes employed in DSSCs. Herein, we synthesized triphenylamine-based dyes bridged by 9,9-di-*n*-octylfluorene-2-vinylene with different conjugation degree to link to the acceptor of cyanoacrylic acid (**Bn**, Chart 1) in order to reveal the relationship between the molecular structures and the performance of DSSCs. It has been found that the total solar-to-energy conversion efficiency of the devices sensitized with **B0**, **B1**, and **B2** are 2.79%, 5.56%, and 4.49%, respectively. It was clear that the cell based on **B1** with balanced conjugated spacer showed a better performance than the one based on **B2**. The reason might be that the electron recombination process from the conduction of TiO₂ to the redox electrolyte was retarded in **B1**-based cell. Therefore, the organic dye with balanced conjugation is important in improving the performance of DSSCs.

* Corresponding author. Tel.: +86 431 88499179; fax: +86 431 88923907; e-mail address: luran@mail.jlu.edu.cn (R. Lu).

2. Results and discussion

2.1. Syntheses of Bn

The synthetic routes for triphenylamine-based dyes (**Bn**, $n=0, 1, 2$) are sketched in Scheme 1. The compounds of 4-(*N,N*-diphenylamino)benzaldehyde (**1**) and 3-(4-diphenylaminophenyl)-2-cyanoacrylic acid (**B0**) were synthesized according to the reported procedures.^{26,22} The precursors of compounds **4** and **6** were prepared by alternate Heck and Wittig reaction.^{23a} For example, *N*-phenyl-*N*-(4-vinylphenyl)benzenamine (**3**) was obtained via Wittig reaction between methyltriphenylphosphoniumiodine and compound **1** in a yield of 89%. Then, compound **4** was readily synthesized from compound **3** and 2-bromo-7-formyl-9,9-di-*n*-octylfluorene (**2**), which was an important intermediate for the whole synthetic process and prepared in accordance with the literature,^{27,28} via Heck reaction catalyzed by Pd(OAc)₂ at 110 °C for 10 h in a yield of 72%. The Wittig reaction between compound **4** and methyltriphenylphosphoniumiodine afforded compound **5** in a yield of 87%. Accordingly, we gained compound **6** from compounds **5** and **2** following the general procedure for compound **4** in a yield of 73%. Finally, the dyes **B1** and **B2** were prepared by Knoevenagel reaction between cyanoacetic acid and compound **4** or **6**, respectively, in a yield of 90% and 92%. All the intermediates and the final products were purified by column chromatography followed by recrystallization, and the new compounds were characterized with FT-IR, ¹H NMR, ¹³C NMR, elemental analysis, and MALDI/TOF mass spectroscopy. The compounds **4**, **5**, **6**, **B1**, and **B2** exhibited vibration absorption bands around 960 cm⁻¹ arising from the wagging vibration of the *trans*-double bond (C=C) in the IR

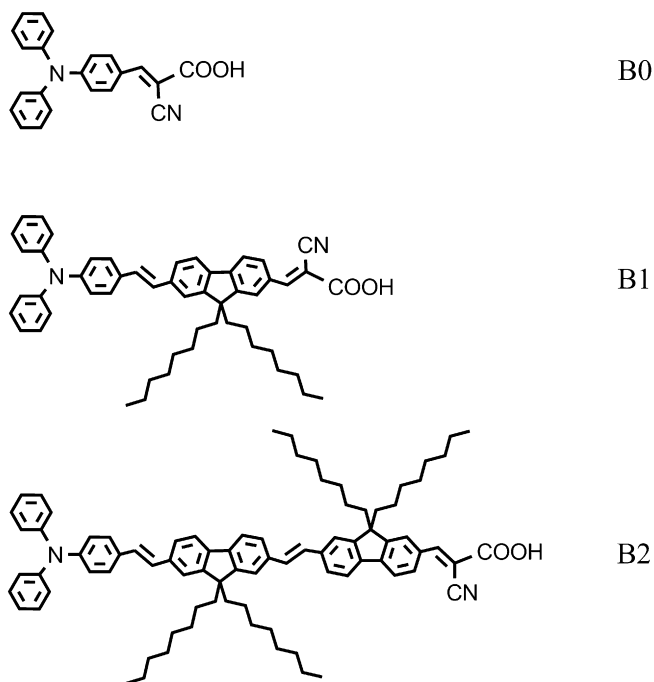
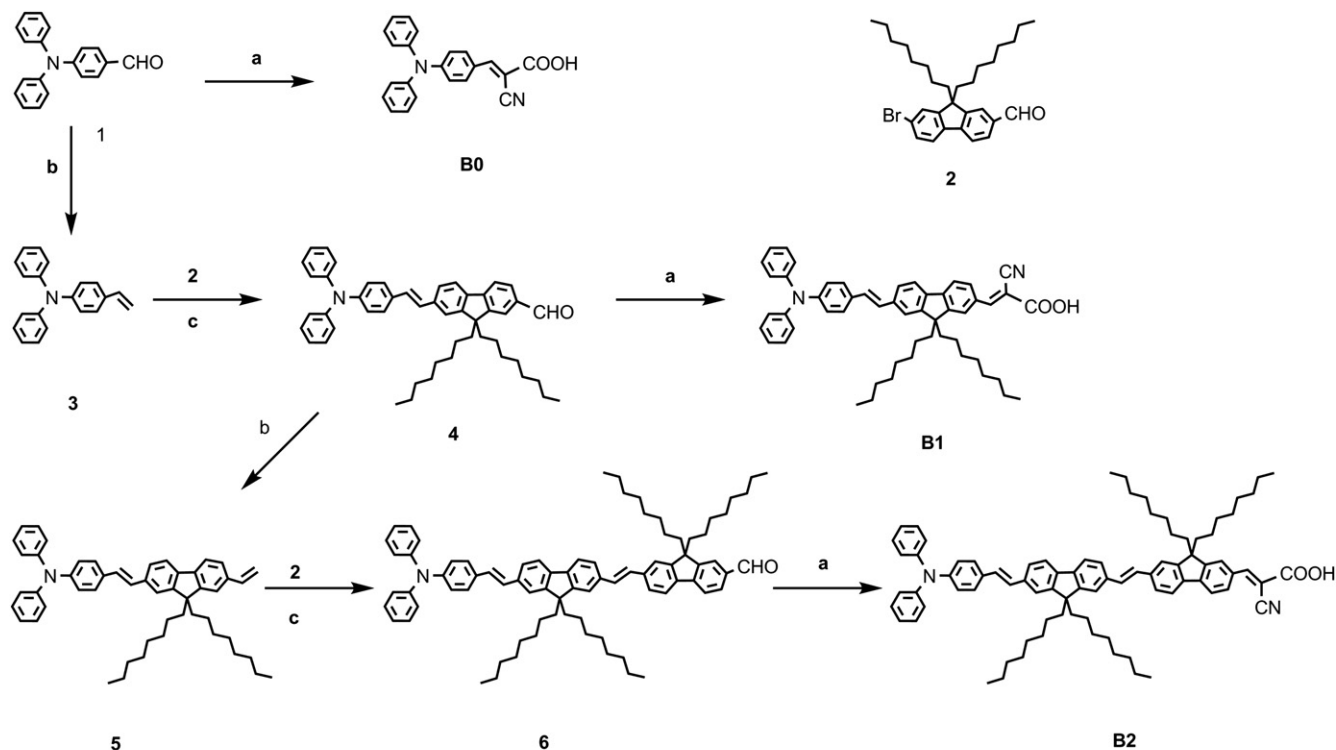


Chart 1. The molecular structures of triphenylamine-based dyes **Bn**.



(a) NH₄OAc, HOOCCH₂CN, CH₃COOH, 135°C, 24h; (b) [Ph₃PCH₃]⁺I⁻, t-BuOK, THF, 0 °C, rt; (c) Pd(OAc)₂, K₂CO₃, DMF, Bu₄NBr, 110 °C, 10 h.

Scheme 1. Syntheses of fluorenylvinylene bridged triphenylamine-based dyes **Bn**.

spectrum.²⁹ In addition, the ¹H NMR spectra of **B1** and **B2** also confirmed that all the ethenyl groups adopted the *trans*-conformation on account of the absence of the signal at ~6.5 ppm assigned to the protons in *cis*-double bonds (CH=CH).^{28,29} The dyes **B0**, **B1**, and **B2** are highly soluble in aromatic solvents (i.e., toluene, benzene, and *o*-dichlorobenzene) and other common organic solvents (such as, CH₂Cl₂, THF, CHCl₃, DMF, and DMSO).

2.2. Photophysical properties

The UV–vis absorption spectra of triphenylamine-based dyes **Bn** ($n=0, 1, 2$) in dichloromethane and on TiO₂ film are shown in Fig. 1, and the photophysical data are listed in Table S1. As shown in Fig. 1a, we can find two distinct absorption at ca. 300 nm and

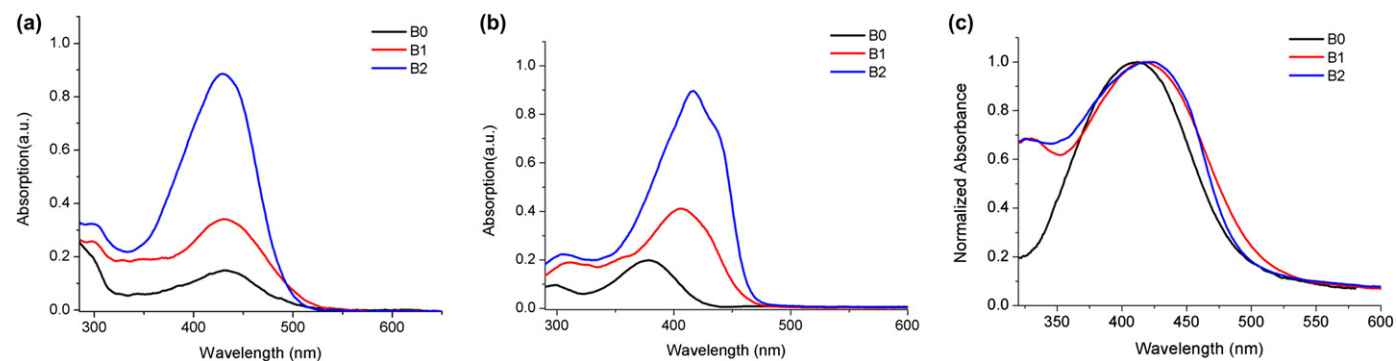


Fig. 1. UV–vis absorption spectra of **Bn** (a) in dichloromethane (2.0×10^{-5} M), (b) in dichloromethane (2.0×10^{-5} M) upon addition of TBAOH, (c) on TiO₂ film (normalized).

430 nm in CH₂Cl₂, and the former one is assigned to π – π^* transition, while the later one originates from the intramolecular charge transfer (ICT) transition.^{23c} However, we can not find that the absorption bands red-shift with increasing the molecular conjugation, which might be due to different degree of protonation of **Bn** in

created because of its partial deprotonation in the excited state,^{21,32} which could be supported by the blue-shift (ca. 20 nm) of the CT bands for **B1** and **B2** in deprotonated forms (cyanoacrylic acid salts) compared with those in protonated forms (cyanoacrylic acid) in THF and toluene (Fig. 2).

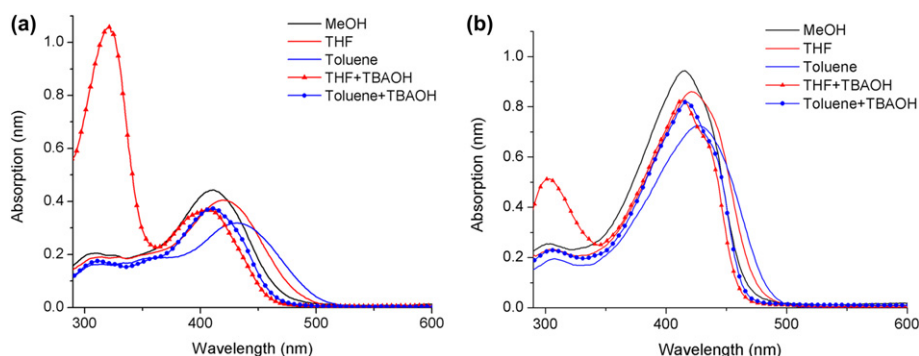


Fig. 2. UV–vis absorption spectra of **B1** (left) and **B2** (right) in different solvents before and after addition of TBAOH.

dichloromethane.^{17,30} Moreover, in order to confirm the above conclusion, the UV–vis absorption spectra of the deprotonated **Bn** are given in Fig. 1b. The deprotonation of **Bn** was achieved by adding TBAOH (tetrabutylammonium hydroxide) to the corresponding solutions. It was clear that the absorption maximum red-shifted obviously with increasing the number of fluorenevinylene unit in **Bn**. For instance, the maximal absorption bands for **B0**, **B1**, and **B2** were located at 378, 406, and 417 nm, respectively. In addition, the absorption spectra of **Bn** adsorbed on transparent TiO₂ films (2 μ m in thickness) are shown in Fig. 1c. The absorption maximum for **B0**, **B1**, and **B2** appeared at 412, 418, and 422 nm, respectively, giving blue-shift compared with those in CH₂Cl₂,

2.3. Molecular orbital calculations

Density functional theory (DFT) calculations method was performed to analyze the electron distribution of the frontier orbitals of dyes **B1** and **B2**. As shown in Fig. 3, the electron density of the highest occupied molecular orbitals (HOMOs) of the both molecules is mainly located at the triphenylamine moieties, whereas electron density of the lowest unoccupied molecular orbital (LUMO) is primarily located at the cyanoacrylic acid acceptor and the neighboring fluorene ring. Therefore, the strong electron density relocation between HOMO and LUMO is present and supports an intramolecular charge transfer (ICT) transition.⁷ Furthermore,

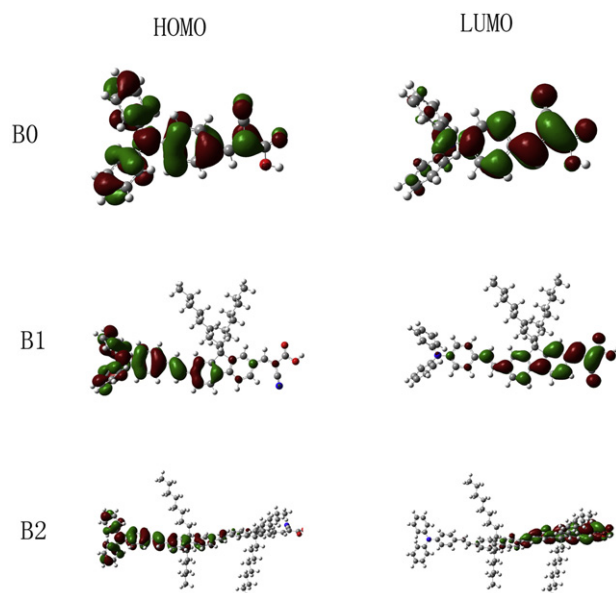


Fig. 3. The frontier orbital plots of the HOMO and LUMO of **Bn**.

the calculated electron distribution illustrates favorable directionality for injection of photoexcited electrons from the donor group to TiO_2 film via the bridge of fluorenylvinylenes and anchoring group.

2.4. Electrochemical properties

To estimate the HOMO level of the dyes, cyclic voltammetry was employed using a three-electrode cell and an electrochemistry workstation (CHI 604). The cyclic voltammetry (CV) diagrams of dyes **Bn** ($n=0, 1, 2$) in methylene chloride (DCM) in the presence of Bu_4NBF_4 as the supporting electrolyte are shown in Fig. 4, and the corresponding data are listed in Table S2. It is shown that the first oxidation potentials (E_{ox}) corresponding to the HOMO levels of the dyes (**B0**: 1.21 eV, **B1**: 0.91 eV, **B2**: 0.93 eV) are sufficiently more positive than the I^-/I_3^- redox potential value (0.4 V vs NHE), indicating that the oxidized dyes formed after electron injection into the conduction band of TiO_2 could accept electrons from I^- thermodynamically. The LUMO levels of these dyes (calculated by $E_{\text{ox}} - E_{0-0}$, see Table S2) are more negative than E_{cb} (conduction-band-edge energy level) of the TiO_2 electrode (-0.5 V vs NHE),¹

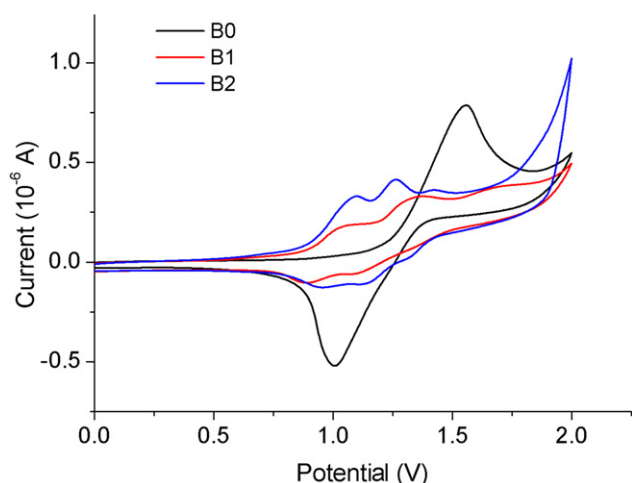


Fig. 4. The cyclic voltammograms of dyes **Bn**, scan rate = 50 mV s^{-1} , versus Fc^+/Fc .

hence, an effective electron transfer from the excited dye to the TiO_2 is ensured.

2.5. Photovoltaic properties of DSSCs

Fig. 5 shows the photocurrent density–photovoltage (I – V) curves of DSSCs based on the as-synthesized dyes, and the detailed parameters, including short-circuit photocurrent density (J_{sc}), open-circuit photovoltage (V_{oc}), fill factor (ff), and conversion effi-

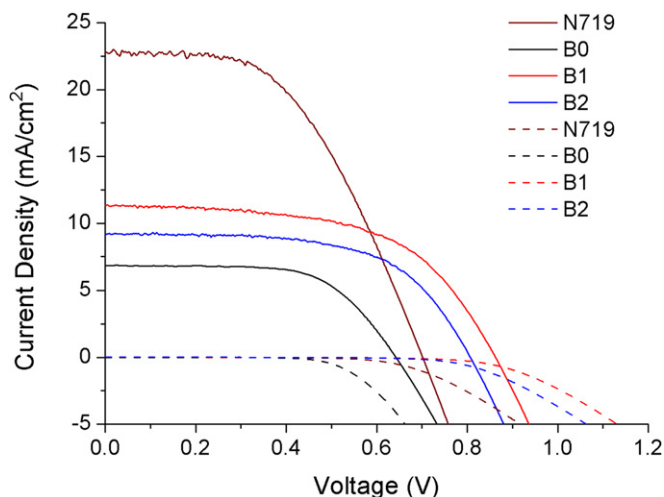


Fig. 5. Current density–voltage curves under full sunlight (real) (AM 1.5 G, 100 mW cm^{-2}) and in the dark (dashed) of devices sensitized with **Bn** and **N719** using a volatile electrolyte.

ciency (η), are summarized in Table 1. The DSSC based on dye **B1** shows the best performance with an open-circuit voltage of 0.86 V, a short-circuit photocurrent density of 11.33 mA cm^{-2} , and a fill factor of 0.57 under AM 1.5 irradiation (100 mW cm^{-2}). And the corresponding overall conversion efficiency (η) is 5.56%, which reaches $\sim 70\%$ of a **N719**-based DSSC (8.04%) fabricated and mea-

Table 1

Photovoltaic parameters of devices with sensitizers **B0**, **B1**, and **B2** at full sunlight (AM 1.5 G, 100 mW cm^{-2})

Dye	Dye load ^a ($10^{-7} \text{ mol cm}^{-2}$)	V_{oc} (V)	J_{sc} (mA cm^{-2})	ff	η (%)
B0	3.28	0.64	6.88	0.63	2.79
B1	3.03	0.86	11.33	0.57	5.56
B2	3.13	0.81	9.22	0.60	4.49
N719		0.71	22.88	0.49	8.04

^a Amount of the dyes absorbed on TiO_2 film.

sured under the same conditions. The spectra of monochromatic incident-photon-to-current conversion efficiency (IPCE) of the devices are shown in Fig. 6, and the characteristics of the spectral response of the photocurrent is comparable to the absorption spectra of the dyes. The IPCE curve of the cell based on dye **B1** shows the highest plateau from 404 to 496 nm, with a maximum of 81% at 468 nm. However, the lower IPCE response for the device sensitized by **B2** with long conjugation of the bridge of fluorenylvinylenes compared with that of **B1** might originate from the poor injection efficiency.²⁴

In addition, the difference of the IPCE spectra of **Bn**-based cell (Fig. 6) could explain why J_{sc} values of the device are in the order of $J_{\text{scB0}} < J_{\text{scB2}} < J_{\text{scB1}}$. The high V_{oc} value of **B1** indicates that the electron recombination process is retarded more effectively in comparison to that in the device of **B0** and **B2**. In order to confirm this judgment, a dark current test was performed (Fig. 5). By extrapolating

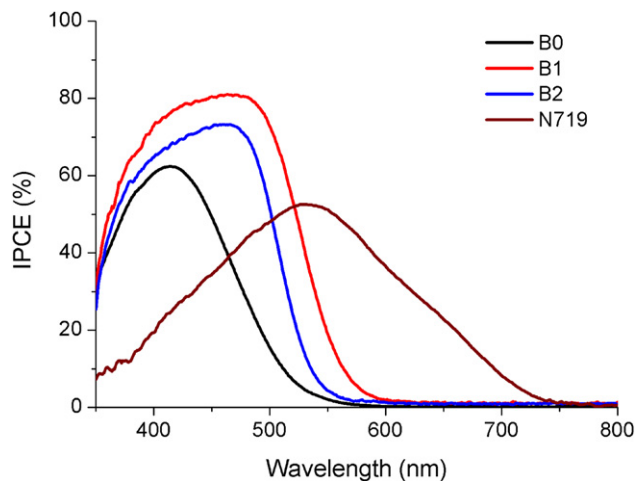


Fig. 6. Incident-photo-to-current conversion efficiency (IPCE) curves of DSSCs sensitized with **Bn** and **N719**.

the high potential region of the $I-V$ curves to $I=0$, the onset potentials of dark currents for the three dyes are estimated as 0.57 V, 0.96 V, and 0.91 V for **B0**, **B1**, and **B2**, respectively. This result suggests that **B1** showed a large dark current and thus suppressed the electron recombination between TiO_2 and I^-/I_3^- redox couple in the electrolyte compared with **B2**.^{23,33}

3. Conclusion

New fluorenylvinylenes bridged triphenylamine-based dyes **Bn** have been synthesized and employed in organic dye-sensitized solar cell. Although a longer conjugation length of the linker may give the increased molar extinction coefficients, the recombination of the photo-induced electrons and triiodide was increased, leading to a lower IPCE response of **B2**-based cell compared with that of **B1**. The maximum photo-to-electrical energy conversion efficiency of 5.56% was achieved in the DSSC based on **B1** under AM 1.5 irradiation (100 mW cm^{-2}). As a result, the introduction of the 9,9-di-*n*-octylfluorene-2-vinylene conjugated spacer can improve the performance of DSSCs efficiently, and the balanced conjugation length of the linker in D- π -A type dyes is of importance in the performance of DSSCs.

4. Experimental section

4.1. Materials and measurements

^1H NMR spectra were recorded on a Mercury plus 500 MHz using CDCl_3 as solvent in all cases. ^{13}C NMR spectra were recorded on a Mercury plus 125 MHz using CDCl_3 as solvent in all cases. UV-vis absorption spectra were determined on a Shimadzu UV-1601PC spectrophotometer. Photoluminescence (PL) spectra were carried out on a Shimadzu RF-5301 luminescence spectrometer. IR spectra were measured using a Germany bruker vertex 80v FT-IR spectrometer by incorporating samples in KBr disks. Mass spectra were performed on Agilent 1100 MS series and AXIMA CFR MALDI/TOF (Matrix assisted laser desorption ionization/Time-of-flight) MS (COMPACT). C, H, and N elemental analyses were taken on a Perkin-Elmer 240C elemental analyzer. Cyclic voltammetry (CV) was performed using CHI 604B electrochemical working station in DCM containing 0.1 M Bu_4NBF_4 as a supporting electrolyte at room temperature. Platinum button and platinum wire were used as a working electrode and a counter electrode, respectively. The potentials were recorded

versus Ag/AgCl (saturated) as a reference electrode. The scan rate was maintained at 50 mV s^{-1} . The thickness of the film was measured using Veeco Dektak 150 Surface Profiler. Ether and tetrahydrofuran (THF) were distilled over sodium and benzophenone. DMF was distilled from phosphorous pentoxide, and other chemicals were used as received without further purification.

4.2. Synthetic procedures and characterizations

4.2.1. 3-(4-(Diphenylamino)phenyl)-2-cyanoacrylic acid (**B0**). Compound **B0** was synthesized according to the corresponding literature procedures.²² Mp: 195.0–197.0 °C. ^1H NMR (500 MHz, CDCl_3) δ : 8.14 (s, 1H), 7.88 (d, $J=9.0$ Hz, 2H), 7.31–7.39 (m, 4H), 7.14–7.24 (m, 6H), 6.97 (d, $J=9.0$ Hz, 2H). IR (KBr, cm^{-1}): 3062, 3036, 2961, 2931, 2873, 2211, 1672, 1585, 958, 826, 761. Elemental analysis calculated for $\text{C}_{22}\text{H}_{16}\text{N}_2\text{O}_2$: C, 77.63; H, 4.74; N, 8.23. Found: C, 77.72, H, 4.56, N, 8.27.

4.2.2. *N*-Phenyl-*N*-(4-vinylphenyl)benzenamine (**3**). Potassium *tert*-butoxide 2.60 g (23.2 mmol) was added to a solution of 11.6 g (28.6 mmol) triphenylmethylphosphonium iodine in 50 mL dry THF at 0 °C. After the mixture was stirred for 15 min at room temperature, 6.50 g (24.0 mmol) 4-(*N,N*-diphenylamino)benzaldehyde (**1**) was added at 0 °C. And the mixture was stirred at room temperature for another 3 h, it was then poured into 400 mL water. The solid was collected by filtration. The crude product was recrystallized in ethyl alcohol to give a white solid in a yield of 89%. Mp: 91.0–92.0 °C. ^1H NMR (500 MHz, CDCl_3) δ : 7.28 (d, $J=8.5$ Hz, 2H), 7.23–7.26 (m, 4H), 7.09 (d, $J=8.0$ Hz, 4H), 6.98–7.03 (m, 4H), 6.63–6.69 (m, 1H), 6.63 (d, $J=16.5$ Hz, 1H), 5.15 (d, $J=8.5$ Hz, 1H). IR (KBr, cm^{-1}): 3085, 3061, 3033, 3003, 2976, 1625, 1592, 992, 841, 760. Elemental analysis calculated for $\text{C}_{20}\text{H}_{17}\text{N}$: C, 88.52; H, 6.31; N, 5.16. Found: C, 88.49, H, 6.43, N, 5.17. MS (MALDI-TOF), m/z : calcd: 271.4, found: 270.6 (see Fig. S2).

4.2.3. (*E*)-7-(4-(Diphenylamino)styryl)-9,9-dioctyl-9H-fluorene-2-carbaldehyde (**4**). A mixture of 2.71 g (10.0 mmol) *N*-phenyl-*N*-(4-vinylphenyl)benzenamine (**3**), 4.97 g (10.00 mmol) 2-bromo-7-formyl-9,9-di-*n*-octylfluorene (**2**), 2.76 g (20.00 mmol) anhydrous potassium carbonate, 3.22 g (10.00 mmol) tetrabutylammonium bromide, and 20 mg (0.089 mmol) $\text{Pd}(\text{OAc})_2$ was added into 15 mL anhydrous DMF under N_2 atmosphere. The resulting mixture was stirred at 110 °C for 12 h, and then was cooled to room temperature, followed by poured into 400 mL water with stirring. The mixture was extracted with CH_2Cl_2 (3×50 mL), the organic liquid was combined and washed with brine. After dried with anhydrous MgSO_4 , the solvent was removed. The crude product was purified by column chromatogram (silica gel) with petroleum ether/dichloromethane (4:1) as eluent, and then recrystallized in petroleum ether to give a green solid in a yield of 72%. Mp: 90.0–92.0 °C. ^1H NMR (500 MHz, CDCl_3) δ : 10.05 (s, 1H), 7.86–7.84 (m, 2H), 7.80 (d, $J=7.8$ Hz, 1H), 7.74 (d, $J=7.9$ Hz, 1H), 7.53–7.51 (m, 1H), 7.47 (s, 1H), 7.44–7.41 (m, 2H), 7.30–7.26 (m, 5H), 7.15–7.09 (m, 5H), 7.08–7.02 (m, 4H), 2.10–1.95 (m, 4H), 1.21–0.99 (m, 20H), 0.82–0.78 (m, 6H), 0.70–0.51 (m, 4H) (see Fig. S3). IR (KBr, cm^{-1}): 3057, 3024, 2952, 2926, 2854, 1698, 1602, 1591, 966, 821, 755. Elemental analysis calculated for $\text{C}_{50}\text{H}_{57}\text{NO}$: C, 87.29; H, 8.35; N, 2.04. Found: C, 87.41, H, 8.23, N, 2.17. MS, m/z : calcd: 688.0, found: 687.8 (see Fig. S4).

4.2.4. (*E*)-4-(2-(9,9-Dioctyl-7-vinyl-9H-fluorene-2-yl)vinyl)-*N,N*-diphenylaniline (**5**). According to the synthetic procedure of compound **3**, compound **5** was prepared from **4** and triphenylmethylphosphonium iodine in a yield of 87% as a light blue solid. Mp: 108.0–110.0 °C. ^1H NMR (500 MHz, CDCl_3) δ : 7.63 (t, $J=8.0$ Hz,

2H), 7.47 (d, $J=8.9$ Hz, 1H), 7.45–7.34 (m, 5H), 7.30–7.26 (m, 4H), 7.14–7.10 (m, 6H), 7.09–7.01 (m, 4H), 6.84–6.78 (m, 1H), 5.80 (d, $J=17.5$ Hz, 1H), 5.26 (d, $J=10.9$ Hz, 1H), 2.0–1.97 (m, 4H), 1.22–1.02 (m, 20H), 0.83–0.78 (m, 6H), 0.70–0.62 (m, 4H) (see Fig. S5). IR (KBr, cm^{-1}): 3062, 3029, 2955, 2927, 2852, 1628, 1593, 961, 825, 751. Elemental analysis calculated for $\text{C}_{51}\text{H}_{59}\text{N}$: C, 89.29; H, 8.67; N, 2.04. Found: C, 89.17, H, 8.80, N, 2.11. MS, m/z : calcd: 686.02, found: 685.4 (see Fig. S6).

4.2.5. 7-((E)-2-(7-(4-(Diphenylamino)styryl)-9,9-dioctyl-9H-fluoren-2-yl)vinyl)-9,9-dioctyl-9H-fluorene-2-carbaldehyde (**6**). According to the synthetic procedure of compound **4**, compound **6** was prepared from compound **5** and 2-bromo-7-formyl-9,9-di-*n*-octylfluorene (**2**) in a yield of 73% as a light green solid. Mp: 50.0–52.0 °C. ^1H NMR (500 MHz, CDCl_3) δ 10.03 (s, 1H), 7.85–7.82 (m, 2H), 7.79 (d, $J=7.7$ Hz, 1H), 7.74 (d, $J=7.9$ Hz, 1H), 7.66–7.62 (m, 2H), 7.57–7.55 (m, 1H), 7.53–7.48 (m, 3H), 7.46–7.44 (m, 1H), 7.43–7.37 (m, 3H), 7.27–7.23 (m, 6H), 7.13–7.06 (m, 6H), 7.06–6.99 (m, 4H), 2.07–1.98 (m, 8H), 1.18–1.00 (m, 40H), 0.79–0.75 (m, 12H), 0.68–0.53 (m, 8H) (see Fig. S7). IR (KBr, cm^{-1}): 3058, 3025, 2953, 2927, 2852, 1693, 1602, 1591, 963, 823, 751. Elemental analysis calculated for $\text{C}_{81}\text{H}_{99}\text{NO}$: C, 88.23; H, 9.05; N, 1.27. Found: C, 88.19, H, 8.86, N, 1.41. MS, m/z : calcd: 1102.6, found: 1102.7 (see Fig. S8).

4.2.6. (Z)-2-Cyano-3-(7-(4-(diphenylamino)styryl)-9,9-dioctyl-9H-fluoren-2-yl)acrylic acid (**B1**). A mixture of compound **4** (0.7 g, 1.02 mmol), cyanoacetic acid (2.13 g, 2.50 mmol), ammonium acetate (200 mg, 2.60 mmol) in glacial acetic acid (30 mL) was heated at 135 °C for 24 h. After cooling to room temperature, the mixture was poured into ice water. The resulting precipitate was filtered off and washed with water. The solid was dissolved in EtOAc and washed with brine. The organic phase was dried by anhydrous MgSO_4 , and the solvent was removed. The crude product was purified by column chromatogram (silica gel) with methyl alcohol/dichloromethane (1:10) as eluent to give a yellow solid (690 mg, 90%) as. Mp: 68.0–70.0 °C. ^1H NMR (500 MHz, DMSO) δ 8.00 (d, $J=23.1$ Hz, 2H), 7.89–7.82 (m, 3H), 7.69 (s, 1H), 7.57–7.53 (m, 3H), 7.35–7.29 (m, 5H), 7.20 (d, $J=16.3$ Hz, 1H), 7.09–7.04 (m, 6H), 6.97 (d, $J=8.7$ Hz, 2H), 2.08–1.92 (m, 4H), 1.16–0.97 (m, 20H), 0.75 (t, $J=7.1$ Hz, 6H), 0.61–0.47 (m, 4H) (see Fig. S9). ^{13}C NMR (125 MHz, CDCl_3) δ 155.63, 153.14, 152.15, 151.37, 147.90, 147.36, 139.46, 138.69, 131.77, 130.82, 129.71, 128.92, 127.82, 127.68, 126.03, 125.72, 125.00, 123.86, 123.53, 121.48, 121.17, 120.49, 97.40, 55.71, 40.74, 30.36, 30.12, 30.00, 29.61, 24.27, 22.99, 14.49 (see Fig. S10). IR (KBr, cm^{-1}): 3063, 3031, 2952, 2925, 2853, 2217, 1624, 1591, 962, 825, 752. Elemental analysis calculated for $\text{C}_{53}\text{H}_{58}\text{N}_2\text{O}_2$: C, 84.31; H, 7.74; N, 3.71. Found: C, 84.44, H, 7.65, N, 3.81. MS, m/z : calcd: 755.0, found: 755.0 (see Fig. S11).

4.2.7. 2-Cyano-3-(7-((E)-2-(7-(4-(diphenylamino)-styryl)-9,9-dioctyl-9H-fluoren-2-yl)vinyl)-9,9-dioctyl-9H-fluoren-2-yl)acrylic acid (**B2**). According to the synthetic procedure of compound **B1**, compound **B2** was prepared from compound **6** and cyanoacetic acid in a yield of 92% as a yellow solid. Mp: 104.0–106.0 °C. ^1H NMR (500 MHz, DMSO) δ 7.96 (d, $J=17.4$ Hz, 2H), 7.90–7.83 (m, 3H), 7.81–7.76 (m, 3H), 7.72 (s, 1H), 7.66 (s, 1H), 7.63–7.59 (m, 2H), 7.55 (d, $J=8.7$ Hz, 3H), 7.48–7.40 (m, 2H), 7.36–7.32 (m, 4H), 7.29 (d, $J=16.5$ Hz, 1H), 7.21 (d, $J=16.3$ Hz, 1H), 7.10–7.04 (m, 6H), 6.98 (d, $J=8.7$ Hz, 2H), 2.10–1.98 (m, 8H), 1.14–1.00 (m, 40H), 0.76–0.71 (m, 12H), 0.61–0.51 (m, 8H) (see Fig. S12). ^{13}C NMR (125 MHz, CDCl_3) δ 154.77, 153.09, 152.10, 151.97, 147.99, 147.66, 145.88, 144.32, 141.31, 140.74, 139.85, 138.47, 137.09, 136.58, 132.17, 131.30, 129.98, 129.70, 128.58, 128.13, 127.91, 127.70, 126.27, 125.88, 125.45, 124.91, 124.04, 123.43, 121.43, 121.22, 121.04, 120.46, 120.32, 98.22, 55.75, 55.41, 41.00, 40.69, 32.19, 30.47, 30.12, 29.64, 24.27, 24.18, 23.00, 14.47 (see

Fig. S13). IR (KBr, cm^{-1}): 3059, 3027, 2952, 2926, 2852, 2217, 1625, 1589, 961, 823, 752. Elemental analysis calculated for $\text{C}_{84}\text{H}_{100}\text{N}_2\text{O}_2$: C, 86.25; H, 8.62; N, 2.39. Found: C, 86.32, H, 8.76, N, 2.27. MS, m/z : calcd: 1169.7, found: 1169.9 (see Fig. S14).

4.3. Theoretical calculation methods

The geometrical structures of **Bn** were optimized by employing the density functional theory at the B3LYP/6-31 level with the Gaussian 03W program package.³⁴ Molecular orbitals were visualized using Gaussview.

4.4. Preparation of Bn-absorbed TiO_2 films

FTO glasses (Solar 2.2 mm thickness, 15 Ω/cm^2 , Nippon Sheet Glass) were first cleaned in a detergent solution using an ultrasonic bath for 10 min, and then rinsed with distilled water and ethanol. After UV– O_3 irradiation for 18 min, the TiO_2 paste, which consists of 16.2% of **P25** (NanoTiO_2) and 4.5% of ethyl cellulose in terpineol, was printed on a conducting glass using a screen printing technique and the electrode was kept in a clean box for a few minutes followed by dried for 6 min at 125 °C. This screen-printing procedure with the nanocrystalline- TiO_2 paste was repeated until the thickness reaches 7 μm . The area of the TiO_2 film was 0.24 cm^2 (0.55 cm of diameter). The film was further dried in air at 100 °C for 15 min followed by another 15 min at 150 °C. Then, the film was calcined at 350 °C for 10 min. Finally, the film was treated at 450 °C for 30 min under oxygen atmosphere. The TiO_2 electrodes were immersed in the aqueous of TiCl_4 (40 mM) for 30 min at 70 °C, and then sintered at 500 °C for 30 min. When the temperature was decreased to 100 °C, the electrodes were immersed into the solution of the dye in dry CH_2Cl_2 (0.2 mM) and kept at room temperature for 12 h.

To prepare a counter electrode, a small hole was drilled in an FTO glass (Solar 2.2 mm thickness, 15 Ω/cm^2 , Nippon Sheet Glass). The perforated plate was rinsed with distilled water and ethanol, followed by ultrasonic treatment in 0.1 M HCl solution in isopropanol for 5 min to remove an iron contamination source. The FTO glass was washed by distilled water and ethanol, and then was treated with ultrasound in acetone for 10 min. After the FTO glass was dried by N_2 flow, H_2PtCl_6 paste was printed on a conducting glass using a screen printing technique and the electrode was kept in a clean box overnight, and then was calcined at 400 °C for 10 min to obtain the counter Pt electrode.

A sandwich cell was prepared by using the dye-anchored TiO_2 film as a working electrode and a counter Pt electrode, which were assembled with a hot-melt-ionomer film of Surlyn polymer gasket. The electrodes were tightly held and heated at 120 °C for 25 s to seal the two electrodes in seal machine (DHS-ES2). The aperture of the Surlyn frame was 2 mm larger than that of the area of TiO_2 film and its width was 1 mm. The hole in the counter electrode was sealed by a film of Surlyn. A hole was then made in the film of Surlyn covered on the hole by a needle. A drop of an electrolyte was put on the hole in the back of the counter electrode. It was introduced into the cell via vacuum backfilling. Finally, the hole was sealed using Surlyn film and a cover glass (0.13–0.17 mm of thickness). The edge of the FTO outside of the cell was roughened with sandpaper. An electrolyte solution used was 0.6 M DMPPI (1,2-dimethyl-3-methylimidazolium iodide), 0.1 M LiI, 0.05 M I_2 , 0.5 M TBP (4-*tert*-butylpyridine) and 0.05 mM GUSCN (Guanidine Thiocyanate) in acetonitrile.

4.5. Photovoltaic characterization of DSSCs

Photoelectrochemical data were measured using a 150 W xenon light source that was focused to give 100 mW cm^{-2} , the equivalent of one sun at AM 1.5, at the surface of the test cell. The spectral output of

the lamp was matched with the aid of a Mega-9 AM 1.5 sunlight filter so as to reduce the mismatch between the simulated and the true Solar spectrum.³⁵ The applied potential and measured cell current was measured using a CHI 604B electrochemical working station. A similar data acquisition system was used to control the incident-photon-to-current conversion efficiency (IPCE) measurement. Under full computer control, light from a 250 W halogen lamp was focused through a high throughput monochromator (Omni- λ 150) onto the photovoltaic cell under test. The IPCE values were determined at 2 nm intervals.⁴ The solar-energy-to-electricity conversion efficiency (η) of the DSSCs is calculated from the short-circuit photocurrent density (J_{sc}), the open-circuit photovoltage (V_{oc}), the fill factor (ff) of the cell, and the intensity of the incident light (P_{in}).³⁶

Acknowledgements

This work is financially supported by the National Natural Science Foundation of China (20874034 and 51073068), 973 Program (2009CB939701), and Open Project of State Key Laboratory of Supramolecular Structure and Materials (SKLSSM201102).

Supplementary data

Supplementary data associated with this article can be found, in the online version, at doi:10.1016/j.tet.2011.09.008.

References and notes

- (a) O'Regan, B.; Grätzel, M. *Nature* **1991**, *353*, 737; (b) Grätzel, M. *Nature* **2001**, *414*, 338.
- Nazeeruddin, M. K.; Kay, A.; Rodicio, I.; Humphry-Baker, R.; Müller, E.; Liska, P.; Vlachopoulos, N.; Grätzel, M. *J. Am. Chem. Soc.* **1993**, *115*, 6382.
- Nazeeruddin, M. K.; Zakeeruddin, S. M.; Humphry-Baker, R.; Jirousek, M.; Liska, P.; Vlachopoulos, N.; Shklover, V.; Fisher, C. H.; Grätzel, M. *Inorg. Chem.* **1999**, *38*, 6298.
- Nazeeruddin, M. K.; Pechy, P.; Renouard, T.; Zakeeruddin, S. M.; Humphry-Baker, R.; Comte, P.; Liska, P.; Cevey, L.; Costa, E.; Shklover, V.; Spiccia, L.; Deacon, G. B.; Bignozzi, C. A.; Grätzel, M. *J. Am. Chem. Soc.* **2001**, *123*, 1613.
- Mishra, A.; Fischer, M. K. R.; Bäuerle, P. *Angew. Chem., Int. Ed.* **2009**, *48*, 2474.
- Moreira Goncalves, L.; de Zea Bermudez, V.; Aguilar Ribeiro, H.; Magalhães Mendes, A. *Energy Environ. Sci.* **2008**, *1*, 655.
- Bhawalkar, J. D.; Kumar, N. D.; Zhao, C. F.; Prasad, P. N. *J. Clin. Laser. Med. Surg.* **1997**, *15*, 201.
- Zhang, G. L.; Bala, H.; Cheng, Y. M.; Shi, D.; Lv, X. J.; Yu, Q. J.; Wang, P. *Chem. Commun.* **2009**, 2198.
- Koumura, N.; Wang, Z. S.; Mori, S.; Miyashita, M.; Suzuki, E.; Hara, K. *J. Am. Chem. Soc.* **2006**, *128*, 14256.
- Tiana, H.; Yanga, X.; Chena, R.; Pana, Y.; Li, L.; Hagfeldt, A.; Sun, L. C. *Chem. Commun.* **2007**, 3741.
- (a) Hara, K.; Sayama, K.; Ohga, Y.; Shinpo, A.; Suga, S.; Arakawa, H. *Chem. Commun.* **2001**, 569; (b) Hara, K.; Kurashige, M.; Danoh, Y.; Kasada, C.; Shinpo, A.; Suga, S.; Sayama, K.; Arakawa, H. *New J. Chem.* **2003**, 27, 783.
- (a) Horiuchi, T.; Miura, H.; Uchida, S. *Chem. Commun.* **2003**, 3036; (b) Horiuchi, T.; Miura, H.; Uchida, S. *J. Photochem. Photobiol., A* **2004**, *164*, 29; (c) Horiuchi, T.; Miura, H.; Sumioka, K.; Uchida, S. *J. Am. Chem. Soc.* **2004**, *126*, 12218; (d) Ito, S.; Zakeeruddin, S. M.; Humphry-Baker, R.; Liska, P.; Charvet, R.; Comte, P.; Nazeeruddin, M. K.; Péchy, P.; Takata, M.; Miura, H.; Uchida, S.; Grätzel, M. *Adv. Mater.* **2006**, *18*, 1202.
- Ehret, A.; Stuhl, L.; Spittler, M. T. *J. Phys. Chem. B* **2001**, *105*, 9960.
- Yao, Q. H.; Meng, F. S.; Li, F. Y.; Tian, H.; Huang, C. H. *J. Mater. Chem.* **2003**, *13*, 1048.
- (a) Sayama, K.; Hara, K.; Mori, N.; Satsuki, M.; Suga, S.; Tsukagoshi, S.; Abe, Y.; Sugihara, H.; Arakawa, H. *Chem. Commun.* **2000**, 1173; (b) Sayama, K.; Tsukagoshi, S.; Mori, T.; Hara, K.; Ohga, Y.; Shinpo, A.; Abe, Y.; Suga, S.; Arakawa, H. *Sol. Energy Mater. Sol. Cells* **2003**, *80*, 47.
- (a) Ferrere, S.; Zaban, A.; Gregg, B. A. *J. Phys. Chem. B* **1997**, *101*, 4490; (b) Ferrere, S.; Gregg, B. A. *New J. Chem.* **2002**, *26*, 1155.
- (a) Velusamy, M.; Thomas, K. R. J.; Lin, J. T.; Hsu, Y. C.; Ho, K. C. *Org. Lett.* **2005**, *7*, 1899; (b) Thomas, K. R. J.; Hsu, Y. C.; Lin, J. T.; Lee, K. M.; Ho, K. C.; Lai, C. H.; Cheng, Y. M.; Chou, P. T. *Chem. Mater.* **2008**, *20*, 1830.
- Kim, S. H.; Choi, H. B.; Baik, C.; Song, K. Y.; Kanga, S. O.; Ko, J. *Tetrahedron* **2007**, *63*, 11436.
- (a) Chen, C. H.; Hsu, Y. C.; Chou, H. H.; Thomas, K. R. J.; Lin, J. T.; Hsu, C. P. *Chem.—Eur. J.* **2010**, *16*, 3184; (b) Choi, H.; Lee, J. K.; Song, K.; Kang, S. O.; Ko, J. *Tetrahedron* **2007**, *63*, 3115; (c) Jung, I.; Lee, J. K.; Song, K. H.; Song, K.; Kang, S. O.; Ko, J. *J. Org. Chem.* **2007**, *72*, 3652; (d) Huang, S. T.; Hsu, Y. C.; Yen, Y. S.; Chou, H. H.; Lin, J. T.; Chang, C. W.; Hsu, C. P.; Tsai, C.; Yin, D. J. *J. Phys. Chem. C* **2008**, *112*, 19739; (e) Ning, Z.; Tian, H. *Chem. Commun.* **2009**, 5483; (f) Ning, Z.; Zhang, Q.; Pei, H.; Luan, J.; Lu, C.; Cui, Y.; Tian, H. *J. Phys. Chem. C* **2009**, *113*, 10307; (g) Satoh, N.; Nakashima, T.; Yamamoto, K. *J. Am. Chem. Soc.* **2005**, *127*, 13030; (h) He, J. X.; Wu, W. J.; Hua, J. L.; Jiang, Y. H.; Qu, S. Y.; Li, J.; Long, Y. T.; Tian, H. *J. Mater. Chem.* **2011**, *21*, 6054; (i) Zhu, W. H.; Wu, Y. Z.; Wang, S. T.; Li, W. Q.; Li, X.; Chen, J.; Wang, Z. S.; Tian, H. *Adv. Funct. Mater.* **2011**, *21*, 756; (j) Tang, J.; Wu, W. J.; Hua, J. L.; Li, J.; Li, X.; Tian, H. *Energy Environ. Sci.* **2009**, *2*, 982; (k) Qu, S.; Wu, W.; Hua, J.; Kong, C.; Long, Y.; Tian, H. *J. Phys. Chem. C* **2010**, *114*, 1343; (l) Song, J.; Zhang, F.; Li, C.; Liu, W.; Li, B.; Huang, Y.; Bo, Z. *J. Phys. Chem. C* **2009**, *113*, 13391.
- Hwang, S.; Lee, J. H.; Park, C.; Lee, H.; Kim, C.; Park, C.; Lee, M. H.; Lee, A.; Park, J.; Kim, K.; Park, N. G.; Kim, C. *Chem. Commun.* **2007**, 4887.
- Lin, J. T.; Chen, P. C.; Yen, Y. S.; Hsu, Y. C.; Chou, H. H.; Yeh, M. C. *P. Org. Lett.* **2009**, *11*, 97.
- (a) Liang, M.; Wu, W.; Cai, F.; Chen, P.; Peng, B.; Chen, J.; Li, Z. *J. Phys. Chem. C* **2007**, *111*, 4465; (b) Xu, W.; Peng, B.; Chen, J.; Liang, M.; Cai, F. *S. J. Phys. Chem. C* **2008**, *112*, 874.
- (a) Hagberg, D. P.; Marinado, T.; Karlsson, K. M.; Nonomura, K.; Qin, P.; Boschloo, G.; Brinck, T.; Hagfeldt, A.; Sun, L. C. *J. Org. Chem.* **2007**, *72*, 9550; (b) Liang, M.; Xu, W.; Cai, F. S.; Chen, P. Q.; Peng, B.; Chen, J.; Li, Z. M. *Angew. Chem.* **2009**, *121*, 1604; (c) Liang, Y. L.; Peng, B.; Liang, J.; Tao, Z. L.; Chen, J. *Org. Lett.* **2010**, *12*, 1204; (d) Ning, Z. J.; Fu, Y.; Tian, H. *Energy Environ. Sci.* **2010**, *3*, 1170.
- (a) Wang, M. K.; Xu, M. F.; Shi, D.; Li, R. Z.; Gao, F. F.; Zhang, G. L.; Yi, Z. H.; Humphry-Baker, R.; Wang, P.; Zakeeruddin, S. M.; Grätzel, M. *Adv. Mater.* **2008**, *20*, 4460; (b) Zhang, G. L.; Bai, Y.; Li, R. Z.; Shi, D.; Wenger, S.; Zakeeruddin, S. M.; Grätzel, M.; Wang, P. *Energy Environ. Sci.* **2009**, *2*, 92.
- Liu, Q.; Liu, W. M.; Yao, B.; Tian, H. K.; Xie, Z. Y.; Geng, Y. H.; Wang, F. S. *Macromolecules* **2007**, *40*, 1851.
- Hagfeldt, A.; Grätzel, M. *Acc. Chem. Res.* **2000**, *33*, 269.
- (a) Zhou, H. P.; Lu, R.; Zhao, X.; Qiu, X. P.; Xue, P. C.; Liu, X. L.; Zhang, X. F. *Tetrahedron Lett.* **2010**, *51*, 5287; (b) Todd, M.; Li, W. J.; Yu, L. P. *J. Am. Chem. Soc.* **1997**, *119*, 844; (c) Heck, H. F.; Nolley, J. P. *J. Org. Chem.* **1972**, *37*, 2320.
- (a) Li, B. S.; Li, J.; Fu, Y. Q.; Bo, Z. S. *J. Am. Chem. Soc.* **2004**, *126*, 3430; (b) Li, B.; Xu, X.; Sun, M.; Fu, Y.; Yu, G.; Liu, Y.; Bo, Z. S. *Macromolecules* **2006**, *39*, 456.
- Qiu, X. P.; Lu, R.; Zhou, H. P.; Zhang, X. F.; Xu, T. H.; Liu, X. L.; Zhao, Y. Y. *Tetrahedron Lett.* **2007**, *48*, 7582.
- Nomura, K.; Morimoto, H.; Imanishi, Y.; Ramhani, Z.; Geerts, Y. J. *Polym. Sci., Part A: Polym. Chem.* **2001**, *39*, 2463.
- Yen, Y. S.; Hsu, Y. C.; Lin, J. T.; Chang, C. W.; Hsu, C. P.; Yin, D. J. *J. Phys. Chem. C* **2008**, *112*, 12557.
- Xu, M. F.; Wenger, S.; Bala, H.; Shi, D.; Li, R. Z.; Zhou, Y. Z.; Zakeeruddin, S. M.; Grätzel, M.; Wang, P. *J. Phys. Chem. C* **2009**, *113*, 2966.
- Markus, K. R.; Fischer, S. W.; Wang, M. K.; Mishra, A.; Zakeeruddin, S. M.; Grätzel, M.; Bäuerle, P. *Chem. Mater.* **2010**, *22*, 1836.
- Wang, Z.; Cui, Y.; Dan-oh, Y.; Kasada, C.; Shinpo, A.; Hara, K. *J. Phys. Chem. C* **2007**, *111*, 7224.
- Frisch, M. J.; Trucks, G. W.; Schlegel, H. B.; Scuseria, G. E.; Robb, M. A.; Cheeseman, J. R.; Montgomery, J. A., Jr.; Vreven, T.; Kudin, K. N.; Burant, J. C.; Millam, J. M.; Iyengar, S. S.; Tomasi, J.; Barone, V.; Mennucci, B.; Cossi, M.; Scalmani, G.; Rega, N.; Petersson, G. A.; Nakatsuji, H.; Hada, M.; Ehara, M.; Toyota, K.; Fukuda, R.; Hasegawa, J.; Ishida, M.; Nakajima, T.; Honda, Y.; Kitao, O.; Nakai, H.; Klene, M.; Li, X.; Knox, J. E.; Hratchian, H. P.; Cross, J. B.; Bakken, V.; Adamo, C.; Jaramillo, J.; Gomperts, R.; Stratmann, R. E.; Yazyev, O.; Austin, A. J.; Cammi, R.; Pomelli, C.; Ochterski, J. W.; Ayala, P. Y.; Morokuma, K.; Voth, G. A.; Salvador, P.; Dannenberg, J. J.; Zakrzewski, V. G.; Dapprich, S.; Daniels, A. D.; Strain, M. C.; Farkas, O.; Malick, D. K.; Rabuck, A. D.; Raghavachari, K.; Foresman, J. B.; Ortiz, J. V.; Cui, Q.; Baboul, A. G.; Clifford, S.; Cioslowski, J.; Stefanov, B. B.; Liu, G.; Liashenko, A.; Piskorz, P.; Komaromi, I.; Martin, R. L.; Fox, D. J.; Keith, T.; Al-Laham, M. A.; Peng, C. Y.; Nanayakkara, A.; Challacombe, M.; Gill, P. M. W.; Johnson, B.; Chen, W.; Wong, M. W.; Gonzalez, C. and Pople, J. A. Gaussian: Wallingford CT, 2004.
- Kamat, P. V.; Haria, M.; Hotchandani, S. *J. Phys. Chem. B* **2004**, *108*, 5166; Xu, W.; Peng, B.; Chen, J.; Liang, M.; Cai, F. *J. Phys. Chem. C* **2008**, *112*, 874.